MULTIBODY DYNAMICS 2011, ECCOMAS Thematic Conference
J.C. Samin, P. Fisette (eds.)
Brussels, Belgium, 4-7 July 2011

MULTIBODY SIMULATION OF SCALED ROLLER-RIG FOR WHEEL/RAIL DEGRADED ADHESION TESTS

F. Bartolini[⋆], R. Conti[⋆], M. Malvezzi[†], E. Meli[⋆], L. Pugi[⋆] and A. Rindi[⋆]

[⋆]Department of Energy Engineering
University of Florence, via S. Marta n. 3, 50139 Firenze, Italy
e-mail: conti@mapp1.de.unifi.it,
web page: http://www.unifi.it/mdmlab

[†]Department of Information Engineering
University of Siena, via Roma n. 56, 53100 Siena, Italy
e-mails: malvezzi@dii.unisi.it

Keywords: Scaled roller-rig, Multibody model, 3D Adhesion model

Abstract. *Modern railways increasingly require equipment that allows to obtain higher performance (in terms of speed, safety and traffic capacity). The design and integration of such components need a deep and careful testing activity. Generally, on modern high-speed trains, complex interactions between traction and low adhesion conditions have to be investigated. A possible solution is the realization of dedicated test-rig, able to reproduce the conditions that the train would meet during a real working condition. In some previous works the feasibility of degraded adhesion tests on a fullscale locomotive roller-rig was investigated. The realization of a fullscale test-rig involves high economical and resources investments; then, in order to perform preliminary tests, a scaled roller-rig has been designed and realized. Beside the roller-rig main design features, a 3D multibody model of the rig and the bogie was developed. The roller rig control strategy requires the on line estimation of the torque applied by the vehicle traction motors; this estimation has to be performed on the basis of the force and angular speed measures, obtained by sensors on the rig. Several errors may affect the reliability of the torque estimator like sliding between roller and wheel, lateral motion and dynamical imbalance of the roller/wheel. Some numerical tests and some preliminary experiments showed that the dynamical imbalance might play an important role in the quality of the torque estimation. The principal purpose of this paper is to realize a complete model of the HIL system with particular attention to the contact model and the analysis of the system behavior when different disturbances are modeled. On the basis of these observations the roller rig multibody model was updated in order to reproduce in a more realistic way the error sources. The numerical tests showed that the control procedure proposed in some previous works was not sufficiently robust with respect to the imbalances; thus a new estimation procedure, based on passband filter, was designed and verified.*

1 Introduction

Scaled roller-rigs [11][13] play an important role in the development of new technologies in railway applications since they represent a trade-off between the standalone numerical simulations and the fullscale roller-rig [3][4][5][6], in terms of economic and time resources. In particular, in Hardware in the Loop (HIL) test-rigs the component to be tested is surrounded with a software/hardware environment; a software core calculates in real time what the components would feel if it were in a real operation and the hardware reproduces, by means of actuators, the control action. Moreover, the scaled roller-rig has to be able to simulate the complex dynamical behavior of the train with low adhesion conditions.

The designed roller-rig is able to perform longitudinal dynamics simulations with high adhesion or with degraded adhesion, (during traction/braking phases, involving the wheel sliding protection and antiskid device) and lateral dynamics.

The main objective of this paper is to develope a complete model of the HIL system in MATLAB®-Simulink® environment (including multibody model of the roller-rig, the model of the train, the controller and the sensors) in order to study new controller strategies and to make preliminary tests. The attention was focused on the disturbance modeling that imposes the development of a more realistic contact model. In [2], beside the roller-rig main design features, a three dimensional multibody model of the rig and the bogie is presented where the attention is focused on a wheel/roller contact model derived from the wheel/pair model [7][8][9]. The new contact model presents some innovative feature, like a complete 3D simulation of the contact phenomena between two revolute surfaces and the possibility to support variable step solvers (with an high improvement of the numerical efficiency).

In order to reduce the setting up phase, the developed control strategy [1] requires the on line estimation of the torque in terms of wheel angular velocities and tangential components of the contact forces. Several errors may affect the reliability of the torque estimator: sliding between the roller and the wheelset may affect the wheel angular acceleration estimation, lateral motion may influence both the relative kinematics between wheel and roller and the contact forces and dynamical imbalance in the roller or in the wheelset could significantly affect the torque estimation. In this work, authors modeled these disturbances updating the multibody dynamic model presented in [11]. Some numerical simulations presented in this paper showed that the dynamical imbalance might play an important role in the quality of the torque estimation.

A series of simulations were performed to investigate the sensitivity of the measure errors on the estimation procedure and to analyze the dynamical behavior of the roller-rig. The numerical tests showed that the architecture proposed in [1] is not robust with respect to dynamical imbalance; thus a new estimation procedure is designed and tested. The new estimation procedure uses a passband filter in order to eliminate the disturbances produced by the dynamical imbalance. The main problem of this disturbance is that the signal is a function of the angular speed; for this reason, the new strategy involves a multi-state approach that discretizes the frequency spectrum of the signal in finite intervals and associates to each discrete interval a filter specifically designed to work in that frequency range.

This paper is organized as follows: section 2 summarizes the general architecture of the roller-rig model, section 3 shows the developed multibody model, and in particular focuses on the 3D wheel-roller contact model and the filter strategy, while section 4 presents and discusses some numerical simulations.

2 Architecture of the Model

The purpose of the railway bogie scaled roller-rig is to reproduce on a scaled test-rig the train dynamical behavior in low adhesion conditions [11][13]. In order to reach this goal, Hardware In the Loop (HIL) [1] approach is used: a virtual train model with a simplified adhesion model simulates the desired vehicle dynamics; then the test rig rollers are controlled in order to simulate the dynamical behavior of the vehicle in terms of wheel angular velocity and torque. In [1] the feasibility of degraded adhesion tests on a HIL full scale roller-rig is discussed.

A railway vehicle usually consists of two bogies, four wheelsets, one carbody and the primary and the secondary suspensions; therefore to reproduce the vehicle dynamics, a fullscale roller-rig has to be composed by the same components. The MDM roller-rig is designed to reproduce the vehicle dynamics but the hardware part allows to test only a single scaled bogie. Consequently, to simulate a whole vehicle a second roller-rig is necessary: this second scaled roller-rig is implemented via software by means of simplified model. In this way the dynamical behavior of the whole railways vehicle can be simulated by using only a scaled roller rig and therefore reducing the building costs of the hardware part. The general architecture of the model is schematically shown in the block diagram of Fig. (1):

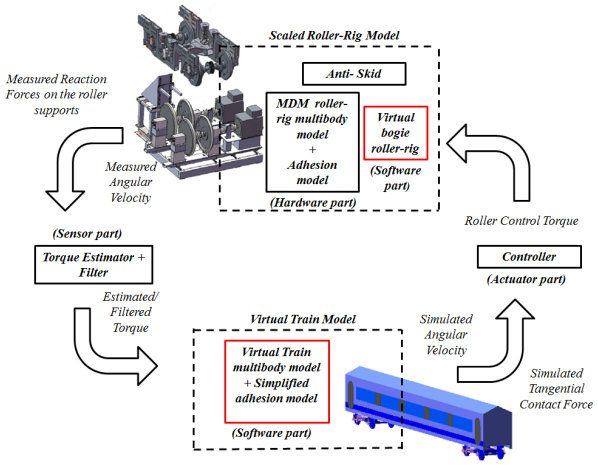

Figure 1: Architecture of the Hardware in the Loop (HIL) Model

This scheme shows the Hardware in the Loop (HIL) approach, where it is possible to define the four fundamental parts of a generic HIL diagram: the *hardware part*, the *software part*, the *sensors* and the *actuators*. Referring to Fig. (1), the Scaled Roller-Rig model represents the hardware part that communicates with the Virtual Train model (the software part) by means of sensors (the Torque Estimator and the Filter). The actuators are the part that contains the controller of the rollers.

The purpose of this paper is to define a realistic multibody model of the MDM roller-rig in order to entirely implement the scheme above in MATLAB®- Simulink®environment. Using this generic subdivision of the HIL system, the four parts are now explained in detail:

1. **Scaled Roller-Rig** (Hardware part): The scaled roller-rig consists of two different models, in order to simulate the whole railway vehicle roller-rig:

   - *MDM scaled roller rig*: Multibody model of the MDM scaled roller-rig [9][12] is composed by the bogie model and the roller model. The bogie model includes the bogie, an half

carbody, two wheelsets and the primary/secondary suspensions. To simulate the contact between wheels and rollers an advanced three-dimensional adhesion model is used [2][7][8]. This block simulates the dynamics of the hardware part of the scaled roller-rig.

- *Virtual bogie roller-rig*: The virtual bogie roller-rig allows to model the second bogie of the vehicle with a simplified analytic virtual model in order to simulate the whole vehicle behavior.

2. **Virtual train model** (Software part): The virtual model is the model of the train used to simulate the vehicle behavior on the rail in different adhesion conditions. This multibody model is a part of the roller-rig control system and then has to be designed for a real-time implementation. Simplified adhesion model is used by the model to simulate various adhesion conditions, including the degraded one.

3. **Controllers** (Actuators part): The aim of the controllers is to reproduce on the roller-rig the same dynamical behavior of the virtual train model in terms of wheel angular velocity and torque [1][12].

4. **Estimators/Filters** (Sensors part): The data that can be measured by the sensors installed on the MDM roller rig are the roller angular velocities and the reaction forces on the roller supports. The estimator block allows to evaluate an estimation of the creep forces and the wheel angular acceleration in order to estimate the torque applied by the bogie motor on the wheel [1]. The filter block reduces noises and disturbances on the estimated torque [14].

3 Description of the components

The previous generic scheme (see Fig. (1)) can be explained in detail, showing the flow data between the four terms:

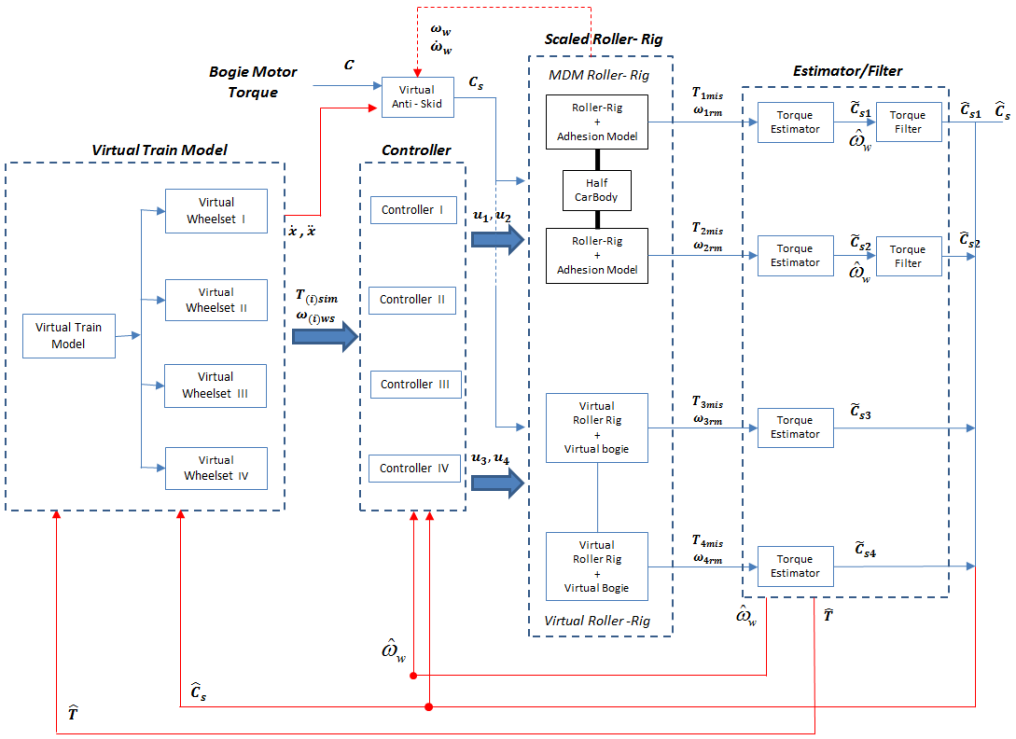

Figure 2: Detailed Architecture of the HIL scheme

3.1 Scaled Roller Rig

3.1.1 MDM Roller Rig: Multibody Model

The main goal is to design a realistic multibody model able to simulate the dynamic behavior of the MDM roller-rig. In literature, some previous works described the design of MDM roller-rig [9][11][13] but all these papers used a simplified model of the MDM roller-rig. The innovation features of this paper with respect to the previous works (that used 2D model) is the development of a complete 3D multibody model of the MDM roller-rig.

The multibody model consists of two parts: the scaled roller-rig and the scaled bogie (with two wheelsets and suspensions). The Scaled Bogie uses the geometric/inertial parameters of the scaled Manchester Wagon [4]. This vehicle has been chosen since it is considered a well known benchmark vehicle model. The multibody model of the bogie on the roller rig is composed by six rigid bodies: the carbody, the bogie, two wheelsets and two rollers; the wheelsets are connected to the bogie by three-dimensional linear/non linear elastic-viscous force elements modeling the primary suspensions, while the bogie is connected to the carbody by three dimensional linear/non linear elastic-viscous force elements reproducing the secondary suspensions. The rollers are constrained to rotate only.
In Fig. (3) is shown a photo of MDM roller-rig produced by SIMPRO while in Fig. (4) a logical scheme of the multibody model is represented.

Figure 3: MDM scaled roller-rig realized by SIMPRO

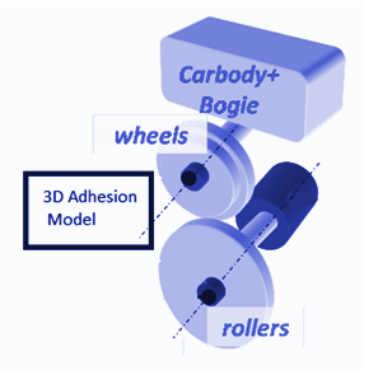

Figure 4: Scheme of the MDM scaled roller-rig multibody model

The main advantage of the scaled test-rig is the reduction of the hardware part costs, compared with the fullscale test rig (see Fig. (1)) but at the same time, increases the time necessary to the design phase since a complete and more complicated analysis of the physical simulated phenomena is required. However, a proper definition of the similitude laws between the scaled model and the real full scale system allows to obtain realistic results and to correctly interpret the experimental data. In literature different approaches are proposed [3]. For the MDM roller-rig, Iwnicky scaling method was chosen; this approach involves several consequences on the system:

- *Time Scaling*: Iwnicki method assures that no scaling is applied to elapsed time and system frequencies; this is an useful feature since the rig is dedicated to HIL simulation. This method allows to maintain the same time and frequency behavior between the real system and the scaled one.

- *Mass-weight mismatch*: Iwnicki method introduces a different scaling factor for mass and weight. For the design of the mechanical part of the rig this is a problem, since weight is proportional

to mass through the gravity acceleration. However, in this paper this problem results not very important because the attention is focused on dynamical simulations and it is possible to solve this issues by means of an offset.

This test-rig is limited in terms of torque erogation and roller angular velocity (that are referred to the standard work condition of the vehicle): the torque is upperly bounded by $20kNm/\phi_T$ (where ϕ_T represents the torque scaling factor) while the angular velocity is limited to 200 rad/s. In order to improve the realistic behavior of the multibody model some physical disturbances (like parameters uncertainty and dynamical axle imbalance) are modeled. The simulated dynamical axle imbalance is calculated in order to reproduce the limits of the regulation in forces [15].

The MDM roller-rig sensors used for the control are the tri-axial load cells, which measures the force reaction on the rollers support and the angular velocity sensors of the rollers. The angular wheel velocity, the angular wheel acceleration and the bogie motor torque have to be evaluated by the estimator block.

3.1.2 MDM Roller Rig: the Wheel/Roller Contact Model

The wheel/roller contact model, that allows to simulate the complete interaction between two revolute surfaces, is an improvement of previous works described in [7][8][10]. The model calculates the creepage forces between the scaled vehicle wheels and the rollers. The wheel-roller interaction model can be logically divide in two parts: the detection of the contact points between two revolute surfaces and the calculation of the contact forces. There are many methods presented in the literature [16][17] to determine the contact point; in this paper the algorithms for the wheel-roller contact point detection is a semi-analytical procedure which presents many innovative features:

- Fully 3D model between two *revolute surfaces*;
- Generic wheel-roller profiles;
- Accurate management of the multiple contact points (without any limit on the multiple solutions);
- High computational efficiency (that allows the online implementability within multibody models).

Before the presentation of this method, the definition of the auxiliary reference systems is necessary. A fixed reference system $O_r x_r y_r z_r$ is defined with its origin located on the roller rotation axis and the axis y_r parallel to the rotation axis (reference Fig. 5). The local reference system $O_w x_w y_w z_w$ is defined on the wheelset with the axis y_w coincident with the rotation axis of the wheelset. The origin O_w coincides with the common point between the nominal rolling plane and the wheelset axis.

The vector $\mathbf{O_w^r}$ defines the position of the local reference system with respect to the fixed one and $[\mathbf{R}]$ is the rotation matrix that represents the relative orientations. In the local system the axle can be described by a revolution surface. The generative function is indicated with $w(y_w)$.

In the local reference frame, the position of a generic point of the wheel surface can be expressed as follows:

$$\mathbf{p_w^w}(x_w, y_w) = [x_w \quad y_w \quad -\sqrt{w(y_w)^2 - x_w^2}]^T. \tag{1}$$

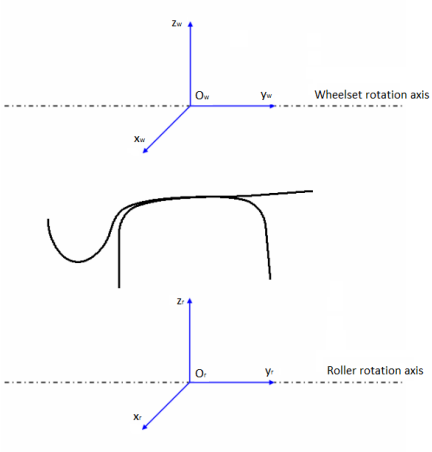

Figure 5: Roller Reference System - Wheel Reference System

In the fixed reference system, the same position is given by the following vectorial expression:

$$\mathbf{p_w^r}(x_w, y_w) = \mathbf{O_w^r} + [\mathbf{R}]\,\mathbf{p_w^w}(x_w, y_w). \tag{2}$$

Similarly the roller can be described by a revolution surface (the generative function is indicated by $r(y_r)$) with respect to the fixed reference system. In this frame, the position of a generic point of the roller surface has the following analytic expression:

$$\mathbf{p_r^r}(x_r, y_r) = [x_r \quad y_r \quad \sqrt{r(y_r)^2 - x_r^2}]^T. \tag{3}$$

The normal unit vector to the wheel surface in the local system is defined by $\mathbf{n_w^w}(\mathbf{p_w^r})$ while, in the fixed reference system, is defined as $\mathbf{n_w^r}(\mathbf{p_w^r}) = [\mathbf{R}]\,\mathbf{n_w^w}(\mathbf{p_w^w})$. In the local reference system, the normal unitary vector is defined to the roller surface as $\mathbf{n_r^r}(\mathbf{p_r^r})$. The method used in this model is based on the idea that the contact points between the wheel surface and the roller surface are located where the distance assumes a stationary point. The following conditions allow to evaluate these points:

- ***1st Condition***: parallelism between the normal unitary vector to the roller surface and the normal unitary vector to the wheel surface $\mathbf{n_r^r}(\mathbf{p_r^r}) \times [\mathbf{R}]\,\mathbf{n_w^w}(\mathbf{p_w^w}) = \mathbf{0}$.
- ***2nd Condition***: parallelism between the normal unitary vector to the roller surface and the vector representing the distance between the generic point of the wheel and the roller $\mathbf{n_r^r}(\mathbf{p_r^r}) \times [\mathbf{R}]\,\mathbf{d^r} = \mathbf{0}$.

Using the reference systems described previously, the distance vector between two generic points belonging to the wheel surface and the roller surface is defined by: $\mathbf{d^r}(x_w, y_w, x_r, y_r) = \mathbf{p_w^r}(x_w, y_w) - \mathbf{p_r^r}(x_r, y_r)$.The distance vector is a function of four parameters.

These conditions could be replaced imposing the orthogonality between the tangent plane to the roller surface and $\mathbf{d^r}(x_w, y_w, x_r, y_r)$ and the orthogonality between the tangent plane to the wheel surface and $\mathbf{d^r}(x_w, y_w, x_r, y_r)$. This formulation results in this case analytically more complicated than the previous one.

The vectorial equations defined in the above conditions represent a system composed by six equations; however only four of them are independent (the first two components of each vectorial equations). The four independent equations of the system can be analytically reduced to a single scalar equation, expressing the variables x_w,x_r and y_r as a function of y_w.

In order to determine x_r, from the second component of the vectorial equation defined by the $1st$ condition of parallelism, the following equation can be found:

$$B\sqrt{A^2 - x_w^2} = Cx_w - D, \tag{4}$$

where

$$A = w(y_w), \tag{5}$$

$$\begin{aligned} B = \quad & -G_x r_{33} - y_w r_{12} r_{33} + w(y_w) w'(y_w) r_{13} r_{32} + \\ & G_z r_{13} + y_w r_{13} r_{32} - w(y_w) w'(y_w) r_{12} r_{33}, \end{aligned} \tag{6}$$

$$C = w(y_w) w'(y_w) r_{11} r_{32} + G_z r_{11} + y_w r_{11} r_{32}, \tag{7}$$

$$D = -G_x w(y_w) w'(y_w) r_{32} + G_z w(y_w) w'(y_w) r_{12}, \tag{8}$$

r_{jk} is the generic element of the rotation matrix $[\mathbf{R}]$ and w' is the wheel profile derivative. The solutions of equation (4) defines the x_w as a function of y_w:

$$x_{w1,2}(y_w) = \frac{CD \pm \sqrt{C^2 D^2 - (C^2 + A^2)(D^2 - A^2 B^2)}}{C^2 + A^2}. \tag{9}$$

From the first component of the $1st$ condition, the following relation can be obtained:

$$r'(y_r)_{1,2} = -\left(\sqrt{1 + \left(\frac{x_r}{\sqrt{r(y_r)^2 - x_r^2}}\right)^2}\right)^{-1} \cdot \frac{x_{w1,2}(y_w) r_{21} - w(y_w) w'(y_w) r_{22} - r_{23}\sqrt{w(y_w)^2 - x_{w1,2}(y_w)^2}}{-w(y_w) w'(y_w) r_{32} - r_{33}\sqrt{w(y_w)^2 - x_{w1,2}(y_w)^2}}. \tag{10}$$

The terms in the denominators are usually not zero, then no other conditions are required. Usually the function $r'(y_r)$ has a descending monotonic trend, therefore $r'(y_r)$ can be numerically inverted in order to obtain $y_{r1,2}(y_w)$, if $r'(y_r)$ is not invertible, a further multiplication of the solution number occurs.

From the second component of the $2nd$ condition, $x_{r1,2}(y_w)$ can be calculated:

$$x_{r1,2}(y_w) = \sqrt{r(y_r)^2 - x_r^2} \cdot \frac{G_x + x_{w1,2}(y_w) r_{11} + y_w r_{12} - r_{13}\sqrt{w(y_w)^2 - x_{w1,2}(y_w)^2}}{G_z + y_w r_{32} - r_{33}\sqrt{w(y_w)^2 - x_{w1,2}(y_w)^2}}. \tag{11}$$

Finally, from the first component of the $2nd$ condition the following scalar equation can be obtained where the unique unknown is y_w:

$$\begin{aligned} F_{1,2}(y_w) = \quad & -r'(y_{r1,2}) r(y_{r1,2}) \left(G_z + y_w r_{32} - r_{33}\sqrt{w(y_w)^2 - x_{w1,2}^2} - \sqrt{r(y_r)^2 - x_r^2}\right) + \\ & -\sqrt{r(y_{r1,2})^2 - x_r^2} \left(G_x + x_{w1,2} r_{11} + y_w r_{12} - r_{13}\sqrt{w(y_w)^2 - x_{w1,2}^2} - y_r\right) = 0. \end{aligned} \tag{12}$$

The solutions $y_{wi}^C \quad i = 1, 2, ..n$ are the coordinates of the contact points. Replacing those values in equations (9)(10)(11) the complete contact point coordinates $(x_{wi}^C, y_{wi}^C, x_{ri}^C, y_{ri}^C)$ with $i = 1, 2, ..n$ can be obtained together with the corresponding contact points on the wheel and on the roller:$\mathbf{p}_{wi}^{r,C} = \mathbf{p}_w^r(x_{wi}^C, y_{wi}^C)$, $\mathbf{p}_{ri}^{r,C} = \mathbf{p}_r^r(x_{ri}^C, y_{ri}^C)$ $i = 1, 2, ..n$. The solution of these equations have to be checked in order to eliminate the phisically meaningless solution; in particular the following conditions are needed :

- *Indentation Condition*: the generic solution $\mathbf{p}_{\mathbf{wi}}^{\mathbf{r,C}}$ can be accepted only if the indentation $p_{ni} = \mathbf{d}_i^{r,C} \cdot \mathbf{n}_r^r(\mathbf{p}_{ri}^{r,C})$ between the wheel surface and the roller surface is negative (with respect to the adopted convection),

- *Convexity Condition*: this condition imposes that the curvature radii of the roller profile have to be smaller than the curvature radius of the wheel profile $k_{1ri}^C + k_{1wi}^C > 0$ and $k_{2ri}^C + k_{2wi}^C > 0$,

- *Analytical Conditions*: the parallelism conditions contain irrational terms, therefore some analytical conditions have to be verified in order to accept the solutions:

  1. the solutions have to be real numbers,
  2. within the parallelism conditions no complex terms have to be present,
  3. the solutions of Eq. (12) have to be effective solutions of the parallelism conditions

The solutions of Eq. (12), that have algebraic multiplicity larger than one, have to be reduced to an unique solution rejecting the other solutions.

For each contact point individuated with the previous method it is necessary to compute the forces and the torque acting on wheelset. The method used in this work consists of two problems: the normal problem and the tangential problem. The normal contact problem, has been solved according to the Hertz theory. Using the Kalker linear theory [16] the tangential contact problem and the spin moment are calculated.

In particular the Hertz'theory allows to evaluate the normal contact force in the contact point:

$$N = k_h |p_n|^\gamma - k_v V_{sl,n}, \tag{13}$$

where V_{sl} is the nominal component of the penetration velocity, p_n is the penetration between roller and wheel and k_h is the Hertz'constants (that depends on materials, contact area, curvatures annd surface) and k_v is the damping contact constant. According to the linear Kalker theory the longitudinal term, lateral component of the tangential force and the spin moment can be evaluated as follows:

$$T_x^* = -f_{11}\varepsilon_x \qquad T_y^* = -f_{22}\varepsilon_y - f_{23}\varepsilon_{sp} \qquad M_{sp} = f_{23} - f_{33}\varepsilon_{sp}, \tag{14}$$

where the four coefficients $f_{11}, f_{22}, f_{23}, f_{33}$ are functions of materials and of the contact area dimension and ϵ_x, ϵ_y, ϵ_{sp} are the creepages. The linear theory of Kalker that is applicable only in case of limited sliding: therefore, to consider the adhesion limit the expression $\sqrt{(T_x^*)^2 + (T_y^*)^2}$ has to be satisfied with the maximum tangential force $T_S = \mu N$. The saturation coefficient is defined by $\xi = \frac{T_s}{T^*}\left[\left(\frac{T^*}{T_s}\right) - \frac{1}{3}\left(\frac{T^*}{T_s}\right)^2 + \frac{1}{27}\left(\frac{T^*}{T_s}\right)^3\right]$ if $T^* \leq 3T_S$ and $\xi = \frac{T_s}{T^*}$ if $T^* > 3T_S$.

The saturated tangential contact forces between wheel and roller in longitudinal and lateral direction are:

$$T_x = \xi T_x^*, \qquad T_y = \xi T_y^*. \tag{15}$$

3.1.3 MDM roller-rig: Simulated Disturbances

The purpose of this paper is to analyze the performance of the controller and the dynamical behavior of the MDM roller-rig when different kind of disturbances are coupled with degraded adhesion condition. The disturbances derive from the model uncertainties that characterize the geometrical/inertial parameters. The disturbances simulated are:

- Bogie longitudinal offset on the MDM roller-rig: this disturbance simulates the uncertainty on the wheel CG (center of gravity) exact position when the bogie is positioned on the MDM roller-rig. In the MDM multibody model it is represented by an alteration of the initial condition between the wheel CG O_w and the roller CG O_r along the x-axis (see Fig. (5)).

- Bogie lateral offset on the MDM roller-rig $G_y(t_0)$: this disturbance causes the bogie hunting on the MDM roller-rig. In the MDM multibody model is represented by an alteration of the initial condition between the wheel CG O_w and the roller CG O_r along the y-axis (see Fig. (5)).

- Dynamical imbalance of the wheelsets and the rollers: the dynamical imbalance of the MDM wheelsets/rollers have to be modeled because there are uncertainties in the exact knowledge of the inertial body parameters and the CG positions. These effects can disturb the controller performance and stability. In literature there is an European standard referring to the wheelsets dynamical imbalance [15]. In the MDM multibody model the mass and the inertial properties of the bodies are modified, in order to simulate a dynamical imbalance.

The dynamical imbalance produces on the wheelset and the roller a nearly sinusoidal disturb that causes on the torque signal, a nearly sinusoidal component. This effect is due to the estimator block, where the estimation of the torque $\widetilde{C}$ is made by estimation the tangential component of the contact force $\widehat{T}$ and the wheel angular acceleration $\widehat{\dot{\omega}}_w$. The dynamical imbalance modifies the estimated torque with a torque disturbance term that can be approximately modeled as follows $C_D(t) = A(t)\sin(\omega(t)t + \phi)$ where $A(t)$ is the amplitude (nearly proportional to the centrifugal term $A(t) \cong mr\omega^2$), $\omega(t)$ represents the angular velocity and ϕ is the phase. The phase term is function of the initial conditions of the system and remains nearly constant in the time.

In this paper a fundamental hypothesis has been made: the *Uncoupled Spectrum Hypothesis*. The spectrum of the torque signal $\tilde{C}_S(t) = \hat{C}_S(t) + C_D(t) + N(t)$ consists of three different contributes: the real torque $\hat{C}_S(t)$, the high frequencies noise $N(t)$ and the torque disturbance $C_D(t)$ as can be see in Fig. (6). The high frequeny noise depends on the measuring noise or

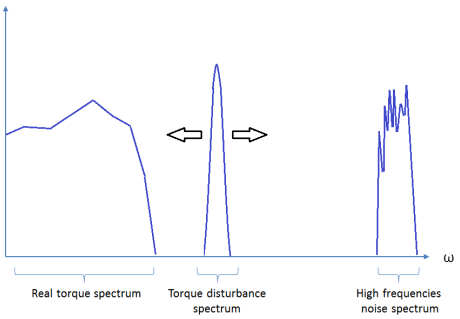

Figure 6: Spectrum of the torque signal

unmodeled dynamics. In this hypothesis, the real torque spectrum has an upper bound of 10Hz. This value is defined considering the frequency work range both of the manual torque control and of the automatic control of the Anti-Skid Device (see Chap. 3.1.4). Since the amplitude

$A(t)$ is variable with the velocity, at low angular speed the error between the real torque and the estimated torque is acceptable, while at high angular speed produces vibrations and modifies the dynamical behavior of the Virtual Train model, for this reason, has to be eliminated. On the contrary, the lower bound of the disturbances is nearly 10 Hz while its upper bound is nearly 200 rad/s due to the maximum train velocity.

3.1.4 Anti-Skid device

The MDM roller-rig allows to reproduce in a realistic way the dynamical behavior of the Virtual Train model. In order to simulate a realistic model of the scaled bogie mounted on the MDM roller-rig, an Anti-Skid device (ASD) is implemented [18]. The Anti-Skid is an electronic device that allows to reduce the slidings between wheel and rig in degraded adhesion conditions. This component uses the informations about the adhesion state in the Virtual Train model to calculate the modulated torque that reduces the slidings. The Anti-Skid works only in traction phase.

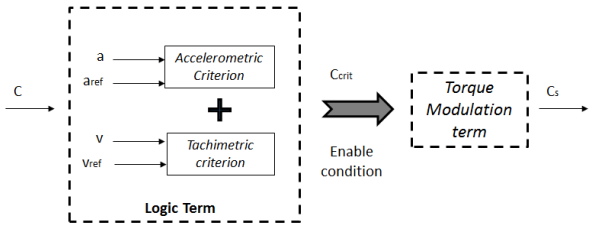

Figure 7: Scheme of the Anti-Skid device

The Anti-Skid model uses the informations obtained from the virtual train model to estimate the adhesion states for each wheelset. The adhesion state is 1 when the wheel losses adhesion and 0 when the wheel is in high adhesion.

The Anti-Skid model consists of two different parts: the logic term evaluates the adhesion state between wheels and rollers comparing the linear velocities and accelerations of the wheels with the virtual train ones, while the modulation term defines the strategy to modulate the torque in order to increase the adhesion between wheel and roller.

The logic term includes two criteria to define the adhesion state between wheel and roller:

- *Speed criterion*: This method compares a threshold value to the velocity error value. This error value is the difference between the linear velocity of the wheels $v = \omega_w r$ and the linear velocity $\dot{x}$ of the virtual train.

- *Accelerometer criterion*: This method compares the acceleration error value to a threshold value. This error value is obtained by difference between the linear acceleration $\dot{v} = \dot{\omega}_w r$ of the wheels and the linear acceleration $\ddot{x}$ of the virtual train.

The two criteria use the logical operator OR to produce the activation signal; therefore the sliding condition can be also activated (or deactivated) by one single criterion. The modulation term defines the action to pass from the loss adhesion state '0' at the full adhesion state '1'; to obtain this result the ASD modulates the torque C_s [18].

3.1.5 Virtual Roller Rig

The purpose of the virtual bogie roller-rig model is to allow to simulate a full vehicle [3] using only a scaled bogie roller-rig like hardware part. In fact, to reproduce the dynamics of the whole vehicle, this approach permits to physically build only one bogie roller-rig and to simulate via software the second virtual bogie roller rig. To improve the computational efficiency of the whole system the virtual roller-rig is modeled by a simplified two-dimensional analytical model. The output are the same of the MDM roller-rig: the measured tangential contact force T_{mis} and the measured roller angular velocity ω_{rm}. The wheel angular acceleration is not evaluated by estimation, but it is directly calculated by the derivation in the estimator block.

3.2 Virtual Train Model

The virtual train model is a simplified 2D model [3] of the longitudinal train dynamics that is used to calculate the linear velocity $\dot{x}$, the linear acceleration $\ddot{x}$ and the load distribution N_i. The operative work hypothesis used in this model are that the train model is bounded in terms of velocity $\dot{x} = \widehat{\omega}_{ws} r$ and motor torque C: the maximum wheel angular velocity is 200 rad/s and the maximum motor torque is 20000 Nm. The virtual train model uses a simplified adhesion model [6] in order to implement this algorithm in a real time software.

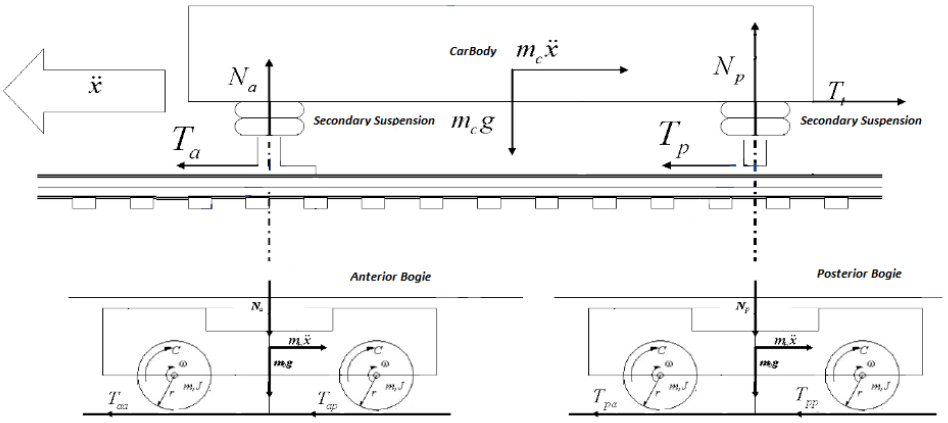

Figure 8: Scheme of the virtual train model

As shown in Fig. (8) the virtual train model consists of two parts:

- *Train block*: this term simulates the longitudinal dynamics of the train on the rig. The model is composed by a carbody, two bogie and four wheelsets; the wheelsets are linked to the bogie by an elastic-viscous force element modeling the primary suspensions. The bogie is connected to the carbody by an elastic-viscous element modeling the secondary suspension. This block allows to calculate the longitudinal acceleration $\ddot{x}$ from the estimated tangential force $\widehat{T}$ and imposing the equilibrium with respect to the pitch rotations, to obtain the load distribution N_1,N_2,N_3 and N_4 on the four axles (in Fig. 8 the scheme is referring to a traction phase). The model has been realized by means of the SimMechanics tool included in the MATLAB®-Simulink®environment.

- *Wheelsets block*: this term is a 2D analytic model of the wheelset which calculates the wheel reference angular velocity ω_{ws} and the reference tangential force T_{sim} from the

normal component of the load N_i, the linear velocity $\dot{x}$ and the estimated torque $\hat{C}_s$ (see Fig. 2):

The separated layout between train and wheelset dynamics allows to obtain a more realistic train model by means of the estimated tangential force $\widehat{T}$ directly estimated on the roller rig. The wheel/rail adhesion model presented in this part of the paper is a simplified model able to manage both pure rolling conditions (micro-sliding) and macroscopic sliding. In order to implement this model in a real-time software, the model has not to be very complicated. The model has been widely described in [1]. The adhesion coefficient $\mu = \mu(\delta)$ is positive during the traction phase and negative during the braking phase. The relative sliding δ is defined by:

$$\delta = \begin{cases} \frac{r\omega - \dot{x}}{max(|r\omega|,|\dot{x}|)} & max(|r\omega|, |\dot{x}|) \neq 0 \\ 0 & r\omega = \dot{x} = 0 \end{cases} \tag{16}$$

where $\dot{x}$ is the linear train velocity, ω is the angular velocity of the wheel and r is the wheel radius. The adhesion function is valid in the range $0 \leq \delta \leq 1$ and it is function of the static and dynamic friction coefficients. These values can be modified in order to simulate different adhesion conditions between the wheel and the rail (for example, including the effects of the environmental conditions).

3.3 Controller

The aim of the controller is to reproduce on the roller rig the same values of angular velocity ω_{ws} and accelerations $\dot{\omega}_{ws}$ which have been calculated by the virtual train model [1][12]. The controller is designed using the sliding mode approach. The control action is the roller motor torque.

The control performances are evaluated observing three parameters:

- *Speed Error* e_ω: error between the simulated wheel angular velocity ω_{ws} and the estimated wheel angular velocity $\widehat{\omega}_w$
- *Torque Estimation Error* e_c: error between the real torque C_S and the estimated torque $\hat{C}_S$
- *Control Torque* u_i: the control torques defined in order to minimize the velocity and torque errors on the MDM roller-rig and the Virtual roller-rig.

The controller consists of two parts, explained in detail in [1]:

- Linear term: this term derives from the dynamical equations of the roller rig and the train model and it is used to generate the control torques in order to produce on the rig the same wheel angular accelerations calculated by the virtual train model. Since in this work a scaled test rig is considered, this part is scaled according to the chosen Iwnicki method and it is defined as $u_{cont} = \frac{R}{r}(C_s(1 - \frac{J_B}{J}\phi_T) + \frac{J_B}{J}T_{sim}r)$.
- Non-Linear term: this term allows to improve the roller rig precision by means of the *sliding mode approach*. This term depends on the difference between the simulated and the measured angular wheel velocity. Furthermore, the non-linear control torque allows to compensate the effects of the not exact knowledge of the real torque C and errors in the estimation of dynamic parameters too. The complete algorithm used in this simulations has been described in previous works and it is defined as $u_{disc} = ksign(\omega_{ws} - \widehat{\omega}_w)$.

3.4 Estimator and Filtering

The aim of the estimator block is to estimate the wheel angular velocity $\widehat{\omega}_w$, the wheel angular acceleration $\widehat{\dot{\omega}}_w$ and the estimated torque of the wheel motor $\tilde{C}$ (see Fig. (2)). These parameters cannot be directly measured because one of the requirements of the scaled roller rig is to reduce the number of sensors mounted on the bogie (in order to reduce the time necessary to the setting up phase in the testing activity). The only outputs of the scaled roller rig that can be measured by the sensors are the roller angular velocity ω_{rm} and the tangential component T_{mis} of the reaction force evaluated in the roller support. Consequently, to evaluate the wheel motor torque the estimator block uses the following equation $\tilde{C} = \widehat{T}r + J_B\widehat{\dot{\omega}}_w$ where $\widehat{T}$ is the estimation of the tangential component of the creepage force $\widehat{T} = T_{mis}$, r is the wheel radius, J_B is the total momentum of inertia of the axle/roller system calculated with respect of wheel rotation axis and $\widehat{\dot{\omega}}_w$ is an estimation of the wheel angular acceleration. In the MDM roller-rig the adhesion condition between wheel and roller is high adhesion condition, therefore, since the rolling radius of the roller is equal to the radius of the wheel, the following estimations for the angular velocity and the angular acceleration can be considered: $\widehat{\omega}_w = -\omega_{rm}$ and $\widehat{\dot{\omega}}_w = -\dot{\omega}_{rm}$.

A reliable value of the wheel motor torque is fundamental for the control system performance. In fact the measured values $\widehat{\dot{\omega}}_w$ and $\widehat{T}$ can be affected by noise/disturbances that may change the dynamical behavior of the MDM roller-rig model.

As said before, the analytical form of the torque disturbance (see Chap. (3.1.3)) considers also the dynamical imbalance of the wheelsets and the rollers in the MDM roller-rig. In order to decrease the time of the setting up phase, a dynamical identification phase is not implemented. Then, the filter strategy has been designed in order to operate in real-time, extracting the disturbance $C_D(t)$ from the torque signal and eliminating the disturbance from the torque. The strategy is based on the spectrum hypothesis and allows to consider the torque signal $\tilde{C}$ composed by the sum of three terms: the real torque$\hat{C}_s(t)$, the high frequency noise $N(t)$ and the torque disturbance $C_D(t)$ $\tilde{C}(t) = \hat{C}_s(t) + C_D(t) + N(t)$.

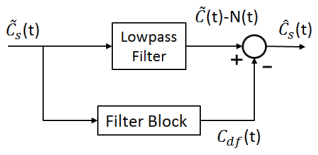

Figure 9: Logical scheme of the filter

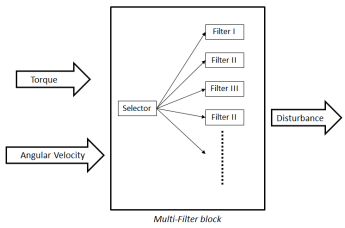

Figure 10: Filter architecture

In order to implement this filter in the model, some specifications are required:

1. Computational efficiency for the HIL simulation: the filter has to run in real-time software.

2. The filtering function has to work in a determinate range of frequencies ([62.8-200 rad/s] due to the *Uncoupled Spectrum Hypothesis*): this specification allows to extract only the disturbance from the torque signal without modifying the real torque.

3. The filter transfer function has not to modify the amplitude and the phase of the disturbance $C_D(t)$: this characteristic is fundamental in order to apply the strategy defined in

Fig. (9), since the on-line elimination of the disturbance from the estimated torque is possible only if the $C_{Df}(t)$ has the same amplitude and the same phase of the $C_D(t)$

4. The filtering function has to be time-variant since the disturbance is function of $\omega(t)$.

The problems was solved using a passband filter that extracts exactly the disturbance $C_D(t)$ imposing conditions both on the amplitude and on the phase of $C_D(t)$: the amplitude has to be unitary while the phase has to be zero. The passband filter is defined by a sixth order elliptic filter because with this filter the performances are reached with medium-low order. The problem with this filter is that the amplitude and phase conditions are valid only in a narrow bound around the cut off frequency of the filter. Therefore, the whole work frequency range [62.8-200 rad/s] has been discretized, a limited number of discrete frequency intervals within which a single filter can guarantee both the amplitude and phase conditions; in other words for each discrete frequency interval, the disturb is filtered by a single passband filter especially designed to work in that discrete range and to satisfy the amplitude/phase conditions. Finally, the selector term starting from the actual angular velocity activates the filter (see Fig. (10)) corresponding to the considered discrete interval.

4 Numerical Simulations

The goal of the numerical simulations is to analyze the behavior of the MDM roller-rig when degraded adhesion condition is present together with different disturbances. The simulated disturbance are:

- Degraded adhesion condition and alteration of the initial condition of the CG Bogie in order to produce hunting (see Chap. (3.1.3)).

- Degraded adhesion condition and dynamical imbalance of the wheelsets and the rollers (see Chap. (3.1.3)).

	Disturbances	**Initial Conditions**	**Control Parameters**
Scenario 1	Bogie lateral offset $G_y(t_0) = 0.0006m$ Low adhesion condition $\mu = 0.05$	$\omega_{init} = 150$ rad/s C increasing ramp	e_c front e_ω front/rear $G_y(t)$
Scenario 2	Wheelsets dynamical imbalance Rollers dynamical imbalance Low adhesion condition $\mu = 0.05$	$\omega_{init} = 150$ rad/s C increasing ramp	e_c front e_ω front/rear

Table 1: Parameters of different Scenarios

The control parameters used to evaluate the system stability and the controller performance are:

1. *Speed Error* e_ω: error between the simulated angular velocity ω_{ws} and the measured angular velocity $\widehat{\omega}_w$.

2. *Torque Estimation Error* e_c: error between the real torque C_S and the estimated torque $\hat{C}_S$. The torque estimation error is referred to the *fullscale model*.

3. *Lateral Displacement* $G_y(t)$: the displacement along the y-axis of the wheel CG. The lateral displacement is referred in the *scaled model*.

The characteristics of the two scenarios proposed in this chapter are summarized in Tab. (1). The torque in the traction phase is modeled by means of a ramp with a delay of 0.5s, with a slope of 5000 Nm/s and limited to 20000 Nm. These values are referred to a generic locomotive working condition.

4.1 Scenario 1

The Scenario 1 purpose is to evaluate the control performances and the dynamical behavior of the MDM roller-rig when low adhesion condition ($\mu = 0.05$) is coupled with a bogie lateral offset ($G_y(t_0) = 0.0006$ m). As said before, the torque applied by the bogie motor is an increasing ramp with a delay; the effect of this torque on the MDM roller-rig is to simulate the train traction phase.

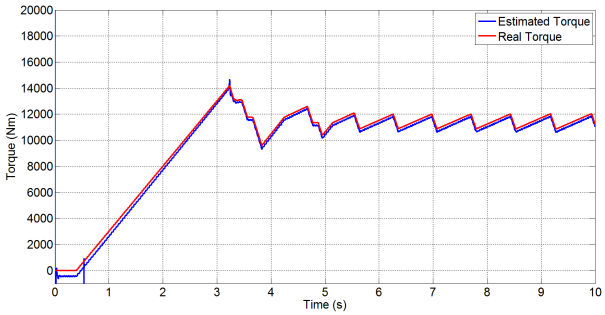

Figure 11: Comparison between the estimated torque $\hat{C}$ and the real torque C on MDM the front wheelset (referred to the fullscale model)

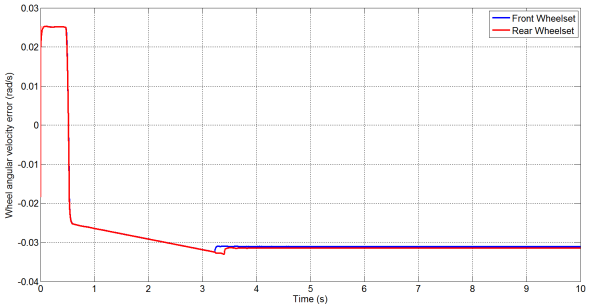

Figure 12: MDM roller-rig: Front/Rear speed error e_ω

The first graphic (see Fig. (11)) shows a comparison between the real torque and the estimated torque for the front wheelset of the MDM roller-rig (referred to the fullscale model). In the steady state, the torque error is nearly 0 ± 200 Nm that is acceptable for the requirements of the system, in terms of controller performance and system stability. In this graphic also the Anti-Skid behavior is evident (see Chap (3.1.4)). The speed error (see Fig. (12)), after a transient period, is stabilized on 0.03 rad/s. The wheelset lateral displacements $G_y(t)$, measured in the scaled model, (see Fig. (13)) shows that, after a transient period, the displacement converges to zero. This figure shows the stability of the whole system and that the controller does not modify the dynamical behavior of the MDM roller-rig. The controller is robust in terms of torque and speed error.

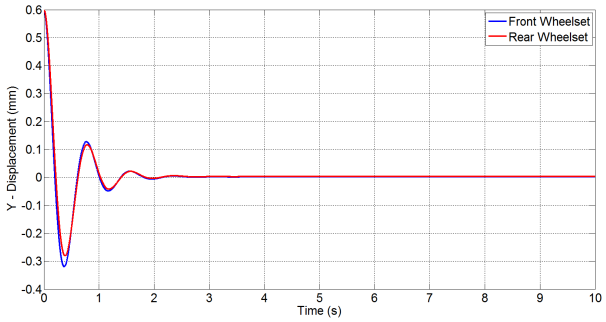

Figure 13: MDM roller-rig: Anterior/Posterior wheelsets lateral displacements G_y (referred to the scaled model)

4.2 Scenario 2

The Scenario 2 purpose is to simulate the dynamical behavior of the MDM roller-rig and the control performances when bad adhesion condition ($\mu = 0.05$) is coupled with wheelset/roller dynamical imbalance [15]. In this scenario two different models are tested: the MDM roller-rig model without Multi-state filter and the MDM roller-rig model with Multi-State Filter (see Chap. (3.4)). The first model allows to show the effects of the dynamical imbalance on the whole system and the second one represents the effects of the Multi-state Filter block on the MDM roller-rig.

4.2.1 Dynamical Imbalance Disturbance Without Multi-filter

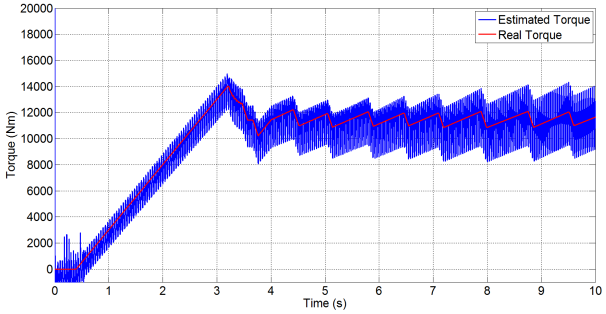

Figure 14: Comparison between the estimated torque $\hat{C}$ and the real torque C on MDM the front wheelset (referred to the fullscale model)

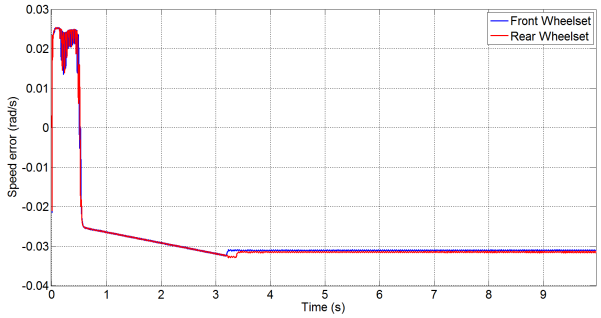

Figure 15: MDM roller-rig: Front/Rear speed error e_ω

As can be seen from the graphics, the presence of the dynamical imbalance produces a disturbance (approximatively sinusoidal) applied on the measured signal. In Fig. (14) the torque behavior is shown: the real torque follows the Anti-Skid algorithm while in the estimated torque the effect of the disturbance $C_D(t)$ (see Chap. (3.4)) is present.

Physically, this disturbance represents a rotating force like the centrifugal force: several numerical simulations have confirmed that a nearly proportional relation between disturbance amplitude $A(t)$ and the centrifugal term exists ($A(t) \cong mr\omega^2$).

The differences are caused by the effect of the 3D adhesion model and inertial imbalance of the wheelsets/rollers bodies. The minimum torque error is 0 ± 1000 Nm and the maximum is 0 ± 2500 that is not acceptable because they are out of range to the system requirements, in terms of controller performance and stability system.

The speed error (see Fig. (15)) after a transient is stabilized nearly on the same value measured in the scenario 1. This result confirms that this controller is robust only with respect the speed error.

4.2.2 Dynamical Imbalance Disturbance With Multi-filter

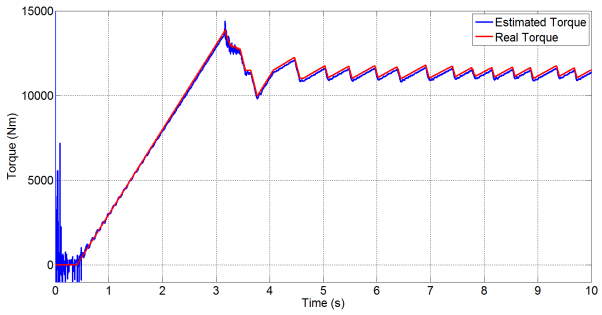

Figure 16: Comparison between the estimated torque $\hat{C}$ and the real torque C on MDM the front wheelset (referred to the fullscale model)

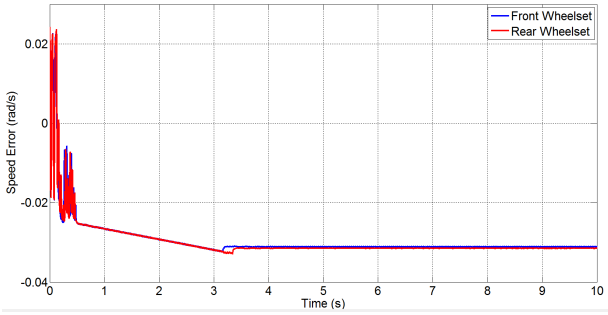

Figure 17: MDM roller-rig: Front/Rear speed error

In this simulation, the filter block (see Chap. (3.4)) has been used. The first figure (see Fig. (16)) shows a comparison between estimated and real torque on the front wheelsets and the great improvement with respect to the Fig. (14) appears clearly: the disturbance $C_D(t)$ is almost filtered. The torque error, after the transient period, is ± 300 Nm and this result is satisfying because this error is very small with respect to the mean torque value (12000 Nm) defined from the Anti-Skid device. The speed error is included in the range limits (see Fig.

(17)). Finally, analyzing Fig. (16) and Fig. (17) it is possible to observe that, with this new estimation procedure, the controller is robust in terms of speed error and torque error.

5 Conclusions and further developments

In this paper a multibody model of the MDM roller-rig was presented, the model was surrounded by the Hardware in the Loop (HIL) architecture, in order to simulate a complete vehicle test-rig. The attention was focused on the sensitivity analysis of the controller with respect some different disturbances. The scaled roller-rig model is completely 3D and allows to simulate different dynamics. In this paper the controller performances was studied, coupling degraded adhesion condition with two different disturbs. The phenomenas simulated were the lateral motion (simulated modifying the initial conditions of the bogie CG and that produces hunting) and the presence of dynamical imbalance on the roller or on the wheel. The contact model presented in this paper represents an improving of those described in previous related works [2][7][8] since this model is fully 3D and allows to determine the contact points between two generic revolute surfaces (wheel and roller).

The numerical simulations concerns two scenarios: the first one analyzes the presence of the lateral motion and the second scenario investigates on the presence of dynamical imbalance on the roller or on the wheel. As can be see from the results relative to scenario 1, a notable lateral motion was simulated in order to produce hunting on the roller-rig. The figures display that the controller is robust with respect lateral motion since the G_y has a damped trend. Moreover, the system is robust in terms of speed error and torque estimation error.

In referring to the presence of dynamical imbalance, some numerical simulations showed that this disturbances influences greatly the torque estimation. The system is robust only in term of speed error. To solve this problem, authors proposed a new method to estimate the torque based on a multi-state filter. In scenario 2, two different cases were compared: without filter and with filter cases. As can be see, in the first case the presence of the disturbance appears clearly in each graphics, modifying the dynamical behavior of the roller-rig and the torque estimation. However, the controller turned out to be very robust in term of wheel angular velocity. The results of the new approach presented, where a multi-state passband filter were implemented to eliminate the disturbance, is shown in the second case: the torque estimation better than the previous one and the controller performances are satisfying. The system in this case is robust in terms of speed error and torque estimation error. As regards the further developments, the definition of a roller motor complete model and the numerical optimization of the contact model are planned. Moreover, the implementation of different disturbances or different initial conditions will be also taken in account.

REFERENCES

[1] M. Malvezzi, B. Allotta and L.Pugi. Feasibility of degraded adhesion tests in a locomotive roller rig. Proceedings of the Institution of Mechanical Engineering, Part F 222, 27–43, 2008.

[2] F. Bartolini, E. Meli, M. Malvezzi, M. Ignesti and L.Pugi. Analysis of the wheel/roller contact problems in the design of a scaled roller rig for the simulation of degraded adhesion conditions. The 1st Joint International Conference on Multibody System Dynamics, May 25-27, 2010, Finland.

[3] A. Jaschinski, H. Chollet, S. Iwnicki. The application of the roller rig to a railway vehicle dynamics. *Vehicle System Dynamics*, **31**, 345–392, 1999.

[4] R. Dukkipati, S. Iwnicki, A. Wickens. Validation of a MATLAB® library vehicle simulation using a roller rig. Tech Report: Manchester Metropolitan University, 1999.

[5] R. Dukkipati. A parametric study of a lateral stability of a railway bogie on a roller rig. Proceedings of the Institution of Mechanical Engineering, Part F, 39–47, 1999.

[6] R. Dukkipati. Lateral stability analysis of a railway truck on a roller rig. Mechanism and Machine theory, 36, 189–204, 2001.

[7] M. Malvezzi, E. Meli, J. Auciello and S. Falomi. Dynamics simulation of a railway vehicles: wheel-rail contact analysis. *Vehicle System Dynamics*, **47**, 867–899, 2009.

[8] M. Malvezzi, E. Meli, A. Rindi and S. Falomi. Determination of wheel-rail contact points with semianalytic method. *Multibody System Dynamics*, **20**, 327–358, 2008.

[9] M. Malvezzi, E. Meli, S. Papini, L. Pugi, M. Rinchi and A. Rindi. A railway vehicle multibody model for real-time applications. *Vehicle System Dynamics*, **46**, 1083–1105, 2008.

[10] E. Meli, M. Malvezzi and L.Pugi. Simulation of degraded wheel-rail adhesion condition on a scaled roller-rig for railway bogies: the effect of wheel-roller contact on control performance. Proceedings of 10th International Conference on Computational Structures Technology, Stirlingshire, Scotland.

[11] B. Allotta, F. Bartolini, L. Pugi and F. Cangioli. A scaled roller test rig for high speed vehicles. *Vehicle System Dynamics*, **48**, 3–18, 2010.

[12] M. Malvezzi, L.Pugi, B. Allotta. Control of a full scale roller rig for the simulation of the wheel sliding. Proceedings of 2007 ASME/IEEE International Conference on Advanced Intelligent Mechatronics, ETH Zurich, Switzerland.

[13] N. Bosso, A. Gugliotta and A. Somà. Progettazione di un banco prova in scala 1/5 per l'analisi sperimentale di carrelli ferroviari. Proceedings of XXIX Congress AIAS, Lucca, Italy.

[14] Oppenheim. *Discrete-Time Signal Processing*. Prentice-Hall, 1989.

[15] UNI-EN 13260. *Wheelsets and Bogies - Product Requirements*. 2009.

[16] J. J. Kalker. *Three - dimensional Elastic Bodies in Rolling Contact*. Kluwer Academic Publishers, 1990.

[17] O. Polach. *Creep forces in simulations of traction vehicles running on adhesion limit*. Wear, 2005.

[18] A. Bassi. Active Anti-Skidding control strategy on electric locomotives. *Railway Traction System Conference*, 87–113, 2001.